

# Anomalously large isotope effect in the glass transition of water

Catalin Gainaru<sup>a</sup>, Alexander L. Agapov<sup>b,c</sup>, Violeta Fuentes-Landete<sup>d</sup>, Katrin Amann-Winkel<sup>d</sup>, Helge Nelson<sup>a</sup>, Karsten W. Köster<sup>a</sup>, Alexander I. Kolesnikov<sup>e</sup>, Vladimir N. Novikov<sup>b,c</sup>, Ranko Richert<sup>f</sup>, Roland Böhmer<sup>a</sup>, Thomas Loerting<sup>d</sup>, and Alexei P. Sokolov<sup>b,c,1</sup>

<sup>a</sup>Fakultät Physik, Technische Universität Dortmund, D-44221 Dortmund, Germany; <sup>b</sup>Department of Chemistry and Joint Institute for Neutron Sciences, University of Tennessee, Knoxville, TN 37996; <sup>c</sup>Chemical Sciences Division and <sup>e</sup>Chemical and Engineering Materials Division, Oak Ridge National Laboratory, Oak Ridge, TN 37831; <sup>d</sup>Institute of Physical Chemistry, University of Innsbruck, A-6020 Innsbruck, Austria; and <sup>f</sup>Department of Chemistry and Biochemistry, Arizona State University, Tempe, AZ 85287

Edited by Pablo G. Debenedetti, Princeton University, Princeton, NJ, and approved October 30, 2014 (received for review June 20, 2014)

We present the discovery of an unusually large isotope effect in the structural relaxation and the glass transition temperature  $T_g$  of water. Dielectric relaxation spectroscopy of low-density as well as of vapor-deposited amorphous water reveal  $T_g$  differences of  $10 \pm 2$  K between  $H_2O$  and  $D_2O$ , sharply contrasting with other hydrogen-bonded liquids for which H/D exchange increases  $T_g$  by typically less than 1 K. We show that the large isotope effect and the unusual variation of relaxation times in water at low temperatures can be explained in terms of quantum effects. Thus, our findings shed new light on water's peculiar low-temperature dynamics and the possible role of quantum effects in its structural relaxation, and possibly in dynamics of other low-molecular-weight liquids.

dynamics of water | isotope effect | quantum effects | glass transition | amorphous ice

Although water is arguably the most important liquid for life, many of its properties remain puzzling (1, 2). In particular, its behavior in the “no-man’s land” between 240 K and 150 K, its low-temperature structural relaxation, and even its glass transition temperature ( $T_g$ ) continue to be topics of active discussion (3–7).

The unusually weak temperature dependence of viscosity near  $T_g \sim 136$  K, estimated indirectly from crystallization rates, has long been known as one of water’s startling features (8). In glass-forming liquids the temperature dependence of viscosity or structural relaxation time  $\tau$  is usually characterized by the fragility index (9):

$$m = \left. \frac{d \log_{10} \tau}{d(T_g/T)} \right|_{T=T_g} \quad [1]$$

Materials such as  $SiO_2$  and  $BeF_2$  display Arrhenius-like  $\tau(T)$  behavior with  $m \sim 20$ – $22$  and are called strong, whereas those with fragility indices  $m \sim 80$  and higher exhibit pronounced super-Arrhenius variations of  $\tau$  and are called fragile. Recent dielectric studies discovered an extremely weak temperature dependence of  $\tau$  in low-density amorphous (LDA) water, with  $m \sim 14$  (10). This is by far the lowest fragility known for any liquid and even below its accepted lower limit,  $m \sim 16$  (9). Recent speculations ascribe this “superstrong” behavior of water to the impact that zero-point quantum fluctuations can have on structural dynamics (7).

Because of the eminent role the atomic mass plays for quantum effects, H/D isotope substitution should have a significant bearing on the low-temperature dynamics of water. To address this question, we performed dielectric measurements on  $H_2O$  and  $D_2O$  prepared as LDA and vapor-deposited water (amorphous solid water, ASW). Details regarding the preparation of LDA water were presented earlier (10) and are briefly summarized in *Materials and Methods* together with ASW preparation, measurements details, and data analysis (for more details, see also

*Supporting Information*). All of the measurements were repeated several times to confirm data reproducibility. The relaxation times  $\tau$  for protonated LDA (H-LDA) water (Fig. 1A) as well as for ASW (Fig. 1B), although differing for the reasons given in *Supporting Information*, both confirm their extremely low fragility,  $m \sim 14 \pm 1$ . An Arrhenius approximation provides estimates of the apparent activation energy  $\sim 34$ – $37$  kJ/mol, with an unusually large pre-exponential factor  $\tau_0 \sim 10^{-10}$  to  $10^{-12}$  s. These parameters reflect an extremely low fragility. Most importantly, LDA water and ASW both reveal an astoundingly strong isotope effect with a  $T_g$  shift of  $\Delta T_g \sim 10 \pm 2$  K between  $H_2O$  and  $D_2O$ , irrespective of the preparation technique (Fig. 1). The size of this effect contrasts with that for other hydrogen-bonded liquids (11, 12) that show  $\Delta T_g \leq 1$  K upon H/D substitution (see also *Supporting Information*).

Previously, differential scanning calorimetry (DSC) studies estimated the isotope shift of water’s  $T_g$  to be  $\Delta T_g \sim 1$ – $3$  K (13, 14), which is significant but smaller than presently found. These DSC measurements were performed using rather high heating rates of  $q \sim 30$  K/min. Can the use of different heating rates be at the origin of this seeming contradiction? To answer this question we performed fixed-frequency dielectric measurements as a function of  $q$ . Akin to the analysis of onset temperatures in DSC, “onset” temperatures were taken as crossing points of two linear extrapolations in Fig. 2 (for details see *Supporting Information*): a low-temperature constant value of  $\epsilon'' = 0$  (horizontal dashed line) and the linear increase with  $T$  (solid line). For both H-LDA

## Significance

Water is by far the most important and intriguing liquid. Despite the relative simplicity of its chemical structure there are many puzzling properties of water that remain the focus of active discussions. Our studies revealed an unusually strong isotope effect and an extraordinarily slow temperature variation of the structural relaxation of water at low temperatures. We show that the anomalous behavior of deeply supercooled water is affected by quantum effects, usually considered negligible for the glass transition. However, in water they are significant owing to the small mass of the molecule. The presented results might considerably change our understanding of water dynamics at low temperatures.

Author contributions: A.L.A., V.N.N., R.R., R.B., T.L., and A.P.S. designed research; C.G., A.L.A., V.F.-L., K.A.-W., H.N., K.W.K., A.I.K., and T.L. performed research; C.G., A.L.A., V.F.-L., K.A.-W., H.N., A.I.K., V.N.N., R.R., R.B., T.L., and A.P.S. analyzed data; and A.L.A., V.N.N., R.R., R.B., T.L., and A.P.S. wrote the paper.

The authors declare no conflict of interest.

This article is a PNAS Direct Submission.

Freely available online through the PNAS open access option.

<sup>1</sup>To whom correspondence should be addressed. Email: sokolov@utk.edu.

This article contains supporting information online at [www.pnas.org/lookup/suppl/doi:10.1073/pnas.1411620111/-DCSupplemental](http://www.pnas.org/lookup/suppl/doi:10.1073/pnas.1411620111/-DCSupplemental).



it should be considered that the slow ramping used for the dielectric experiments, which also show good reproducibility in heating and cooling cycles (*Supporting Information*), provides a more equilibrium-like situation than the fast scanning used in DSC. These results are also consistent with earlier measurements of supercooled water down to  $T \sim 240$  K, which revealed an increasing isotope effect with decreasing temperature, and by extrapolation estimated a  $T_g$  shift of  $\Delta T_g \sim 7$  K (17, 18).

The isotope effect on structure and dynamics of water has been intensively studied at high temperatures and in crystalline ices (19–22). It has been shown that near ambient temperature the difference between  $H_2O$  and  $D_2O$  structure corresponds to a shift in temperature by 5–10 K (19, 20). The liquid’s density maximum shifts by about 7 K (from 3.98 °C to 11.19 °C). At lower temperature quantum effects become more pronounced (19, 20). Earlier studies of dielectric relaxation in crystalline ices at lower temperatures (21, 22) found an isotope shift of more than 10 K, comparable to our observation (Fig. 1). Moreover, our observations on LDA (Fig. 2) are consistent with data collected on crystalline ice in terms of stronger heating rate-dependent relaxation times for  $H_2O$  than for  $D_2O$  (22).

What is the reason for the unusual low-temperature dynamics in water (Fig. 1)? Recently, it was suggested that the superstrong behavior of water’s relaxation might result from quantum effects (7). Water is the molecule with the lowest mass  $M$  existing in the liquid state at ambient conditions, and a possible influence of quantum effects on structure and dynamics of water and ice was emphasized in several papers (22–25). Molecular dynamics simulations demonstrated that quantum effects affect the proton momentum distribution in supercooled water (24), and that they are at the origin of the unusual isotope effect in the thermal expansion of ice (25). The relevance of quantum effects at a temperature  $T$  is usually quantified by the ratio of the thermal wavelength,  $\hbar/\sqrt{k_BMT}$ , to the particle size  $a$ ,  $\Lambda^* = \hbar/\sqrt{k_BMT}/a$ . When  $\Lambda^*$  is  $\sim 0.1$  or larger, quantum effects cannot be neglected (7, 26). Estimates at  $T \sim 136$  K give  $\Lambda^* = 0.06$  for  $H_2O$  and 0.05 for  $D_2O$ , indeed close to 0.1. For comparison,  $\Lambda^*(T_g)$  is  $\sim 0.01$  for propylene glycol and glycerol. Thus, quantum effects are expected to be considerable for water but negligible for most other H-bonding liquids.

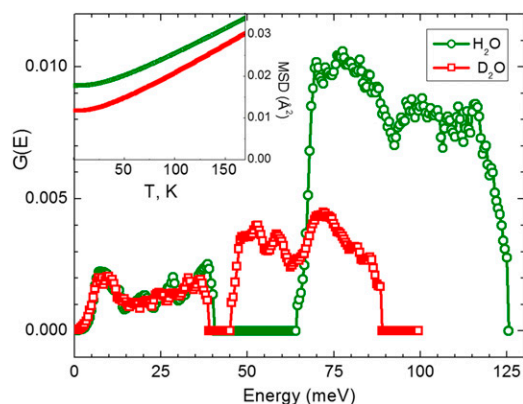


**Fig. 3.** Vibrational density of states  $G(E)$  for H-LDA and D-LDA ice recorded at  $T = 15$  K (28–30). The librational modes at 50–125 meV are displaying a strong isotope effect. (*Inset*) The calculated MSD as a function of temperature for H-LDA and D-LDA using the measured vibrational density of states (details are presented in *Materials and Methods*; see also *Supporting Information*). The zero-point MSD of D-LDA is significantly smaller than that of H-LDA. Hence, at temperatures close to  $T_g$  the zero-point contributions to the total MSD are lower for amorphous  $D_2O$ , leading to weaker quantum effects in comparison with  $H_2O$ .

Direct confirmation for the importance of quantum effects can be obtained by analyzing the atomic mean-square displacement (MSD),  $\langle u^2 \rangle$ . If at a given temperature zero-point quantum fluctuations contribute significantly to  $\langle u^2 \rangle$ , then quantum effects need to be taken into account. The MSD can be estimated from the generalized vibrational density of states,  $G(E)$ , that is accessible via neutron scattering (27). Earlier measurements reported  $G(E)$  for the intermolecular translational bands (0–40 meV) as well as for the librational bands (50–125 meV) of H-LDA and D-LDA (for details see *Supporting Information*) (28–30). These results reveal a clear isotope effect, especially for the librational mode (Fig. 3). Using the  $G(E)$  shown in Fig. 3 we calculated the temperature dependence of the total MSD in the harmonic approximation:

$$\langle u^2 \rangle \propto \int \frac{G(E)}{E} \left[ n(E, T) + \frac{1}{2} \right] dE, \quad [2]$$

which assumes that  $G(E)$  does not change significantly with  $T$ . Here,  $n(E, T) = [\exp(E/k_B T) - 1]^{-1}$  is the Bose population factor. The results (Fig. 3, *Inset*) show indeed that near  $T_g$  zero-point fluctuations contribute significantly to the MSD of LDA water ( $\sim 60\%$  in  $H_2O$  and  $\sim 45\%$  in  $D_2O$ ). To assess the possible impact of zero-point fluctuations on the temperature-dependent relaxation times in water, we use the expression proposed in ref. 31:

$$\log_{10}(\tau/s) = a_0 + a_1 \langle u^2(T_g) \rangle / \langle u^2(T) \rangle + a_2 (\langle u^2(T_g) \rangle / \langle u^2(T) \rangle)^2. \quad [3]$$

Here  $\langle u^2(T_g) \rangle$  is the MSD at  $T_g$ ,  $a_1 = 1.622$ , and  $a_2 = 12.3$  are universal constants and  $a_0 = -1.922$ , assuming  $\tau(T_g) = 10^2$  s. The temperature-dependent relaxation times calculated from Eq. 3 reproduce the fragilities, that is, the slopes of the experimental data, surprisingly well for both  $H_2O$  and  $D_2O$  (Fig. 1A). Disregarding the zero-point contributions to the MSD alters the temperature dependence of  $\tau$  predicted by Eq. 3 significantly and disagrees at least by a factor of 2 with the slope of the experimental data (Fig. 1A). These results suggest that quantum fluctuations indeed play an important role for the dynamics of supercooled water and might be the reason for its unusually low fragility.

Can quantum effects also be at the origin of the large isotope effect in the low-temperature dynamics of water? Assuming that two independent relaxation routes exist, based either on classical barrier crossing or on quantum tunneling, the total relaxation rate can approximately be written as

$$W = \frac{1}{\tau} = W_{cl} + W_{tun} \approx W_0 \exp\left(-\frac{E_a(T)}{k_B T}\right) + W_0 \exp\left(-\frac{2}{\hbar} \int p dx\right). \quad [4]$$

Here  $W_0 \propto M^{-1/2}$  is the attempt frequency,  $E_a(T)$  the activation energy,  $p = [2M(U(x) - E_0)]^{1/2}$  the momentum,  $M$  the mass,  $E_0$  the energy of the tunneling particle, and  $U(x)$  the potential (32). This is a crude approximation for quantum tunneling, because it considers tunneling from a single level  $E_0$ . The total tunneling probability should be taken as an integral of tunneling probabilities from all possible energy levels with their corresponding populations at a given temperature. Nevertheless, we will use this simplistic picture just to get qualitative estimates.

Let us also assume that all interaction parameters and potentials remain invariant and that only  $M$  changes upon isotope substitution. This assumption is supported by diffraction studies that show that the same structural model fits both  $H_2O$  and  $D_2O$  data (33), and that there is no significant difference in the bond lengths between  $H_2O$  and  $D_2O$  (34). Moreover, opposing inter- and intramolecular quantum effects lead to a cancellation of their influence on the strength of the hydrogen bond

(34, 35). Then, the over-barrier relaxation time is affected by the weak mass dependence in the pre-exponential factor,  $W_0$ , and changes by only  $\sim 5\%$ , that is,  $\tau(\text{D})/\tau(\text{H}) \sim 1.05$ . For rotational motions momentum of inertia rather than mass needs to be taken into account and the change in  $\tau$  can be  $\sim 20\text{--}40\%$ . This agrees well with our analysis of propylene glycol and glycerol data that show  $\tau(\text{D})/\tau(\text{H}) \sim 1.1\text{--}1.3$ , largely independent of temperature in the entire range (Fig. 1*B*, *Inset*). Our argument is also confirmed by water data at high temperature (36–38) where over-barrier relaxation should dominate (Fig. 1*B*, *Inset*).

Quantum tunneling, however, depends exponentially on the square root of mass:

$$W_{\text{tun}} \propto \frac{1}{\sqrt{M}} \exp\left[-\sqrt{M} Z(T)\right], \quad [5]$$

with  $Z(T) = 2 \int [2(U(x) - E_0)]^{1/2} dx/\hbar$ . Assuming that quantum effects dominate at water's  $T_g$ , we estimate that  $W_{\text{tun}}(T_g) = 1/\tau(T_g) \sim 10^{-2}$  to  $10^{-3} \text{ s}^{-1}$ , whereas the prefactor  $W_0 \sim 10^{13}$  to  $10^{14} \text{ s}^{-1}$ . This yields  $M^{1/2} Z(T_g) \sim [15\text{--}17] \ln 10 \sim 35\text{--}39$  and implies that  $\tau(\text{D})/\tau(\text{H}) \sim 1.05 \exp[0.05Z(T_g)] \sim 7\text{--}8.5$  (i.e., the relaxation time should increase by 600–750%). An even larger increase might be expected for rotational tunneling. Our experimental data reveal that the relaxation times indeed increase  $\sim 6\text{--}15$ -fold (Fig. 1*B*, *Inset*).

These results suggest that whereas near ambient temperature the dynamics of water is dominated by over-barrier relaxation and exhibits only a weak isotope effect, quantum effects become increasingly important for its structural relaxation as temperature decreases. Indeed, it has been shown (17, 18) that the isotope effect regarding the structural relaxation time, the diffusion, and the viscosity of bulk supercooled water all increase strongly with decreasing temperature and reach  $\tau(\text{D})/\tau(\text{H}) \sim 3$  at  $T \sim 240 \text{ K}$  (Fig. 1*B*, *Inset*). An earlier study of dielectric relaxation of ice also raised the possibility that quantum effects are important (22). An unusual temperature dependence (a decrease in the apparent activation energy with temperature decrease) and a strong isotope effect were also observed in this case. However, the activation energy of the relaxation observed in these ices (21, 22) is higher ( $\sim 45\text{--}50 \text{ kJ/mol}$ ) than the one observed in our case, which probably indicates a different nature of the relaxation process. Interestingly, an activation energy as low as  $\sim 23 \text{ kJ/mol}$  has been reported for relaxation in ice V at  $T < 190 \text{ K}$  (39), which makes this phase a suitable candidate for a search of tunneling phenomena in crystalline ices.

An important implication of the proposed considerations is that quantum effects extend the supercooled regime of  $\text{H}_2\text{O}$  by reducing its  $T_g/T_m$  ratio from the classic value of  $\sim 2/3$  to  $\sim 0.50$  ( $T_m$  is the melting temperature). Furthermore, we demonstrated that quantum behavior can strongly affect water's structural dynamics at  $T \sim T_g$ ; it leads to an unusually low fragility,  $m \sim 14$ , and to the strong isotope effect evident from Fig. 1. According to this scenario, with increasing molecular mass the quantum effects should be mitigated. Indeed, for  $\text{D}_2\text{O}$  the  $\Lambda^*$  parameter and the quantum contributions to the MSD (Fig. 3) both decrease. Consequently, the  $T_g/T_m$  ratio of  $\text{D}_2\text{O}$  increases to  $\sim 0.53$ , closer to the usual value of  $\sim 0.67$ . Molecules of other hydrogen-bonding liquids are significantly heavier and do not exhibit significant isotope effects, that is, the impact of quantum effects on their dynamics is negligible.

To summarize, the proposed quantum effects explain consistently several anomalies of water dynamics: (i) the unusually low value of  $T_g/T_m$ ; (ii) the extraordinarily low fragility,  $m \sim 14$ ; and (iii) the unusually strong isotope effect on  $T_g$  as discovered here. Analyzing the dynamics of other light-molecule liquids might help to unravel how general this behavior is. It is obvious that a detailed theoretical treatment of quantum effects is required. This will advance our understanding of water's structural relaxation even

further and aid in clarifying the role played by quantum fluctuations for the dynamics of low- $T_g$  glass-forming liquids in general.

## Materials and Methods

**Generalized Vibrational Density of States  $G(E)$  Estimated from Neutron Scattering Measurements.** The temperature dependence of the MSD,  $\langle u^2 \rangle$ , for hydrogen (deuterium) atoms in ice has been calculated from the generalized density of vibrational states,  $G(E)$ , which is directly obtained from inelastic neutron scattering (INS). The incoherent INS spectrum is proportional to the density of vibrational states weighted by the squared eigen-vectors  $|e_i(j, E_j)|^2$  for constituent atoms  $i$  of normal vibrational modes  $j$  and energy  $E_j$ , and there are no selection rules for neutron scattering (all modes are active). The INS spectra of LDA water, taken from previous studies (28–30), were measured at 15 K using the time-of-flight spectrometer TFXA (40) at ISIS Spallation Neutron Source. The measured INS spectra were transformed to the dynamical structure factor,  $S(Q, E)$ , where  $Q$  and  $E$  denote neutron momentum and energy transfer, respectively. In general,  $S(Q, E)$  for hydrogen-containing materials can be described by Eq. 6, which includes scattering with absorption  $l$  and creation ( $k-l$ ) of vibrational modes and single- and multiphonon contributions:

$$S(Q, E) = \sum_{l,k} S_{l,k-l}(Q, E) = e^{-\langle u_i^2 \rangle Q^2} \sum_{l,k} \left( \frac{\hbar^2 Q^2}{6m_H} \right)^k \int dE_1 \dots dE_k \frac{G(E_1) \dots G(E_k)}{E_1 \dots E_k (k-l)!} \\ \times \prod_{i=l+1}^k [n(E_i, T) + 1] \prod_{j=1}^l n(E_j, T) \delta \left( E - \sum_{i=l+1}^k E_i + \sum_{j=1}^l E_j \right) \quad [6]$$

$$G(E) = \sum_j |e_H(j, E_j)|^2 \delta(E - E_j) \quad [7]$$

$$\langle u_H^2 \rangle = \frac{\hbar^2}{3m_H} \int \frac{G(E)}{E} \left[ n(E, T) + \frac{1}{2} \right] dE. \quad [8]$$

Here  $m_H$  is the mass of a hydrogen atom,  $n(E_j, T) = [\exp(E_j/k_B T) - 1]^{-1}$  is the Bose population factor, and the summation in Eq. 7 runs over all normal vibrational modes.

Via Eq. 6 the one-phonon neutron scattering contribution was extracted by using the measured spectra and an iterative technique (28, 41). At the first step  $G(E)$  was calculated from Eq. 6 and assuming that in the range up to 125 meV the measured data present the one-phonon spectrum. This spectrum was used then to calculate the two-, three-, and four-phonon neutron scattering contributions using Eq. 6. At the second and subsequent steps, the difference between the experimental spectrum and the calculated multiphonon contribution was accepted as the new one-phonon spectrum. For the analyzed spectra convergence was reached in three iterations. Fig. S1 shows the experimental  $S(Q, E)$  spectrum and the calculated one-phonon and multiphonon contributions for the LDA sample. It can be seen that the multiphonon contribution is small at low energies ( $E < 70 \text{ meV}$ ) and that it increases significantly toward higher energies. Thus, the multiphonon correction of the neutron scattering data are important. The INS single-phonon spectra of water can be separated into two parts owing to intermolecular translational vibrations (below  $\sim 40 \text{ meV}$ ) and librational vibrations (in the range  $\sim 50\text{--}130 \text{ meV}$ ).

### Details of Dielectric Spectroscopy Measurements.

**Measurements of LDA water.** LDA water was investigated dielectrically using an Alpha-A impedance analyzer in combination with a Quatro cryosystem (Novocontrol). Samples of deuterated amorphous ice were prepared as previously described for protonated amorphous ice (10). Owing to uncertainties in estimating the exact filling factor, Fig. S2 gives the dielectric loss in arbitrary units. Prior to each measurement the dielectric cell was transferred to the cryostat, which was precooled at 100 K. To record the data presented in Fig. 2 and Figs. S2 and S3, each sample was initially slowly heated to about 135–140 K until the transition from the high-density to the low-density amorphous phase occurred (10). The temperature was then decreased to about 130 K and the spectra of LDA water were measured while increasing the temperature in steps of 3 K (Fig. S2). During each step, after the temperature was stabilized within 0.1 K, the spectrum was recorded using a nested frequency sweep to check for signs of crystallization during the data acquisition. This was indeed the case at 154 K, as Fig. S2 demonstrates. To determine the time constants for all temperatures the spectra were horizontally shifted so that a master curve (Fig. S2*B*) is constructed on top of the spectrum recorded at 151 K. A similar procedure was applied to assess the dielectric time constants for protonated LDA water (10). The heating rate-dependent measurements (Fig. 2) were done

at a constant frequency 1 Hz on LDA samples prepared in the same way as described above. Details of the measurements and estimates of the onset temperature are presented in [Supporting Information](#).

**Measurements of ASW water.** Dielectric measurements of deposited water were carried out using an interdigitated electrode (IDE) cell (42) (IME 1050.5-FD-Au-U; ABTECH Scientific Inc.). The IDE structure consists of 50 pairs of Au electrode fingers. Each finger has the dimensions of  $4,990 \times 10 \times 0.1 \mu\text{m}^3$  with a spacing of  $10 \mu\text{m}$  between electrodes. The geometric capacitance of the IDE cell was calibrated at room temperature using air, isopropyl alcohol, and water as reference materials. The IDE cell was placed onto a copper holder with silver paint applied between the IDE and the holder to ensure good thermal contact. The holder was mounted onto the cold stage of a closed-cycle He cryostat with high-vacuum sample environment. Temperature stability during the measurements was within  $\pm 0.01$  K of the set point. Dielectric measurements were performed using a Solartron SI-1260 gain-phase analyzer in combination with a Mestec DM-1360 transimpedance amplifier.

Both regular (Chromasolv Plus; Sigma Aldrich) and heavy (AcroSeal, 99.75% minimum deuteration) water samples were deposited onto interdigitated electrodes at  $T = 14$  K at a rate of about 5 nm/s. These conditions result in the formation of an amorphous film (43, 44). The thickness of the deposited film was about 20  $\mu\text{m}$ . After the deposition the film was heated to 148.5 K in the case of  $\text{H}_2\text{O}$  and 158.5 K in the case of  $\text{D}_2\text{O}$  at a rate of 0.4 K/min and annealed at this temperature for 10 min. The measurements of the ASW- $\text{H}_2\text{O}$  sample were performed in the temperature range 148.5–136.5 K in steps of 2-K intervals. For the ASW- $\text{D}_2\text{O}$  sample measurements were performed in the temperature range 158.5–136.5 K with 2-K intervals. Dielectric spectra of ASW- $\text{H}_2\text{O}$  and - $\text{D}_2\text{O}$  samples are presented in [Fig. S4](#).

To ensure that the film was stable in the course of the dielectric experiment it was subsequently measured on the heating cycle in the same temperature range. Temperature ramping between set points on cooling and heating cycles was kept at a low rate of 0.4 K/min to avoid crystallization. The spectra measured on cooling and subsequent heating agree well ([Fig. S5](#)), indicating stability of the sample during the measurements. The onset of crystallization on the heating cycle was observed at temperatures 150–152 K for ASW- $\text{H}_2\text{O}$  and 158–160 K for ASW- $\text{D}_2\text{O}$ : The amplitude was slowly, but irreversibly, decreasing and the width of the relaxation spectrum was increasing at and above the indicated temperature range. The structural relaxation time in ASW

samples was determined from a fit to a Cole–Cole relaxation model at high temperatures, 148.5 K for ASW- $\text{H}_2\text{O}$  and 158.5 K for ASW- $\text{D}_2\text{O}$ . At lower temperatures the relaxation times were determined from the horizontal shift factors obtained using time–temperature superposition. The master curve of the dielectric losses in ASW- $\text{H}_2\text{O}$  measured at different temperatures is demonstrated in [Fig. S6](#).

**Measurements of hydrogenated and deuterated propylene glycol and glycerol.** To check whether the isotope effect in water is indeed anomalous we have measured the effect of H/D substitution for other H-bonding liquids: hydrogenated and deuterated propylene glycol (PG) and glycerol. We used hydrogenated PG ( $\text{C}_3\text{H}_8\text{O}_2$ ) from Sigma-Aldrich (Puriss. p.a., ACS reagent,  $\geq 99.5\%$ ) deuterated PG ( $\text{C}_3\text{D}_8\text{O}_2$ ) from C/D/N Isotope Inc. (98 atom% D), hydrogenated glycerol ( $\text{C}_3\text{H}_8\text{O}_3$ ) from Sigma-Aldrich (spectrophotometric grade,  $\geq 99.5\%$ ), and deuterated glycerol ( $\text{C}_3\text{D}_8\text{O}_3$ ) from Cambridge Isotopes (99 atom % D). For PG isotopic substitution leads to a relative change of the total molecular mass  $\sim 10.5\%$  and for glycerol this change is  $\sim 8.7\%$ , comparable to the  $\sim 11\%$  change for  $\text{D}_2\text{O}/\text{H}_2\text{O}$ . The hydrogenated and deuterated PG and glycerol samples were measured using an Alpha-A impedance analyzer in combination with a Quatro cryosystem (Novocontrol). Analysis of the dielectric relaxation in PG and glycerol reveals a very weak isotope effect with a shift  $\Delta T_g \sim 0.1$  K for PG ( $T_g$  of h-PG is 168.0 K and of d-PG it is 168.1 K) and  $\sim 0.4$  K for glycerol (45) ( $T_g$  of h-glycerol is 189.3 K and of d-glycerol is 189.7 K) ([Fig. S7](#)). Thus, the effect of H/D isotope substitution on the glass transition of water ( $\Delta T_g \approx 10$  K) is significantly stronger than in other hydrogen-bonding materials such as ethanol ( $\Delta T_g \approx 0$  K) (12, 46), PG ( $\Delta T_g \approx 0.1$  K), and glycerol ( $\Delta T_g \approx 0.4$  K) (45).

**ACKNOWLEDGMENTS.** A.L.A. and A.I.K. were supported by the Scientific User Facilities Division, Office of Basic Energy Sciences, US Department of Energy. We also thank NSF Chemistry Division for partial financial support (A.P.S. and V.N.N. acknowledge Grant CHE-1213444 and R.R. acknowledges Grant CHE-1026124). T.L. acknowledges funding by the Austrian Science Fund FWF (START Award Y391 and International Grant I1392) and the European Research Council ERC (Starting Grant SULIWA). K.A.-W. acknowledges funding by the Austrian Science Fund FWF (Firnberg programme T463). Work at Dortmund was partially funded by the Deutsche Forschungsgemeinschaft under Grant BO1301.

- Mishima O, Stanley HE (1998) The relationship between liquid, supercooled and glassy water. *Nature* 396(6709):329–335.
- Angell CA (2008) Insights into phases of liquid water from study of its unusual glass-forming properties. *Science* 319(5863):582–587.
- Ito K, Moynihan CT, Angell CA (1999) Thermodynamic determination of fragility in liquids and a fragile-to-strong liquid transition in water. *Nature* 398(6727):492–495.
- Smith RS, Kay BD (1999) The existence of supercooled liquid water at 150 K. *Nature* 398(6730):788–791.
- Debenedetti PG (2003) Supercooled and glassy water. *J Phys Condens Matter* 15(45):R1669.
- Angell CA (2004) Amorphous water. *Annu Rev Phys Chem* 55(1):559–583.
- Novikov VN, Sokolov AP (2013) Role of quantum effects in the glass transition. *Phys Rev Lett* 110(6):065701.
- Angell CA (1993) Water-II is a strong liquid. *J Phys Chem* 97(24):6339–6341.
- Böhmer R, Ngai KL, Angell CA, Plazek DJ (1993) Nonexponential relaxations in strong and fragile glass formers. *J Chem Phys* 99(5):4201–4209.
- Amann-Winkel K, et al. (2013) Water's second glass transition. *Proc Natl Acad Sci USA* 110(44):17720–17725.
- Singh LP, Richert R (2012) Two-channel impedance spectroscopy for the simultaneous measurement of two samples. *Rev Sci Instrum* 83(3):033903.
- Ramos MA, Talón C, Jiménez-Riobóo RJ, Vieira S (2003) Low-temperature specific heat of structural and orientational glasses of simple alcohols. *J Phys Condens Matter* 15(11):S1007–S1018.
- Johari GP, Hallbrucker A, Mayer E (1990) Isotope effect on the glass transition and crystallization of hyperquenched glassy water. *J Chem Phys* 92(11):6742–6746.
- Elsaesser MS, Winkel K, Mayer E, Loerting T (2010) Reversibility and isotope effect of the calorimetric glass  $\rightarrow$  liquid transition of low-density amorphous ice. *Phys Chem Chem Phys* 12(3):708–712.
- Wang L-M, Velikov V, Angell CA (2002) Direct determination of kinetic fragility indices of glass-forming liquids by differential scanning calorimetry: Kinetic versus thermodynamic fragilities. *J Chem Phys* 117(22):10184–10192.
- Mao C, Chamarthy SP, Byrn SR, Pinal R (2010) Theoretical and experimental considerations on the enthalpic relaxation of organic glasses using differential scanning calorimetry. *J Phys Chem B* 114(11):269–279.
- Qvist J, Mattea C, Sunde EP, Halle B (2012) Rotational dynamics in supercooled water from nuclear spin relaxation and molecular simulations. *J Chem Phys* 136(20):204505.
- Prielmeier FX, Lang EW, Speedy RJ, Lüdemann HD (1988) The pressure dependence of self diffusion in supercooled light and heavy water. *Ber Bunsenges Phys Chem* 92(10):1111–1117.
- Hart RT, et al. (2006) Isotope quantum effects in water around the freezing point. *J Chem Phys* 124(13):134505.
- Bergmann U, et al. (2007) Isotope effects in liquid water probed by x-ray Raman spectroscopy. *Phys Rev B* 76(2):024202.
- Johari GP, Jones SJ (1975) Study of the low-temperature “transition” in ice Ih by thermally stimulated depolarization measurements. *J Chem Phys* 62(10):4213–4223.
- Bruni F, Consolini G, Careri G (1993) Temperature dependence of dielectric relaxation in  $\text{H}_2\text{O}$  and  $\text{D}_2\text{O}$  ice: A dissipative quantum tunneling approach. *J Chem Phys* 99(1):538–547.
- Bove LE, Klotz S, Paciaroni A, Sacchetti F (2009) Anomalous proton dynamics in ice at low temperatures. *Phys Rev Lett* 103(16):165901.
- Morrone JA, Car R (2008) Nuclear quantum effects in water. *Phys Rev Lett* 101(1):017801.
- Pamuk B, et al. (2012) Anomalous nuclear quantum effects in ice. *Phys Rev Lett* 108(19):193003.
- Markland TE, et al. (2011) Quantum fluctuations can promote or inhibit glass formation. *Nat Phys* 7:134–137.
- Marshall W, Lovesey SW (1971) *Theory of Thermal Neutron Scattering* (Clarendon, Oxford).
- Kolesnikov AI, et al. (1997) Neutron scattering studies of vapor deposited amorphous ice. *Phys Rev Lett* 79(10):1869–1872.
- Li J, Kolesnikov AI (2002) Neutron spectroscopic investigation of dynamics of water ice. *J Mol Liq* 100(1):1–39.
- Li J (1996) Inelastic neutron scattering studies of hydrogen bonding in ices. *J Chem Phys* 105(16):6733–6755.
- Larini L, Ottocchian A, De Michele C, Leporini D (2008) Universal scaling between structural relaxation and vibrational dynamics in glass-forming liquids and polymers. *Nat Phys* 4(1):42–45.
- Ankerhold J (2007) *Quantum Tunneling in Complex Systems: The Semiclassical Approach* (Springer, Berlin).
- Bowron DT, et al. (2006) The local and intermediate range structures of the five amorphous ices at 80 K and ambient pressure: A Faber-Ziman and Bhatia-Thornton analysis. *J Chem Phys* 125(19):194502.
- Zeidler A, et al. (2012) Isotope effects in water as investigated by neutron diffraction and path integral molecular dynamics. *J Phys Condens Matter* 24(28):284126.
- Markland TE, Berne BJ (2012) Unraveling quantum mechanical effects in water using isotopic fractionation. *Proc Natl Acad Sci USA* 109(21):7988–7991.
- Kaatz U (1993) Dielectric relaxation of  $\text{H}_2\text{O}/\text{D}_2\text{O}$  mixtures. *Chem Phys Lett* 203(1):1–4.
- Okada K, Yao M, Hiejima Y, Kohno H, Kajihara Y (1999) Dielectric relaxation of water and heavy water in the whole fluid phase. *J Chem Phys* 110(6):3026–3036.
- Collie CH, Hasted JB, Ritson DM (1948) The dielectric properties of water and heavy water. *Proc Phys Soc* 60(2):145–160.
- Johari GP, Whalley E (2001) The dielectric relaxation time of ice V, its partial antiferroelectric ordering and the role of Bjerrum defects. *J Chem Phys* 115(7):3274–3280.

40. Penfold J, Tomkinson J (1986) The ISIS time focused crystal analyser spectrometer TFXA. Report RAL-86-019 (Rutherford Appleton Laboratory, Oxfordshire, UK).
41. Kolesnikov AI, Li JC (1997) Multiphonon contributions in inelastic neutron scattering spectra of ice. *Physica B: Cond. Mat.* 234–236(0):34–36.
42. Yang L, Guiseppi-Wilson A, Guiseppi-Elie A (2011) Design considerations in the use of interdigitated microsensor electrode arrays (IMEs) for impedimetric characterization of biomimetic hydrogels. *Biomed Microdevices* 13(2):279–289.
43. Olander DS, Rice SA (1972) Preparation of amorphous solid water. *Proc Natl Acad Sci USA* 69(1):98–100.
44. La Spisa S, et al. (2001) Infrared and vapor flux studies of vapor-deposited amorphous and crystalline water ice films between 90 and 145 K. *J Geophys Res Planets* 106(E12): 33351–33361.
45. Wang L-M, Tian Y, Liu R, Richert R (2010) Structural relaxation dynamics in binary glass-forming molecular liquids with ideal and complex mixing behavior. *J Phys Chem B* 114(10):3618–3622.
46. Krivchikov AI, Bermejo FJ, Sharapova IV, Korolyuk OA, Romantsova OO (2011) Deuteration effects in the thermal conductivity of molecular glasses. *Low Temp Phys* 37(6):517–523.